Comparison of the Binding of Glucose and Glucose 1-Phosphate Derivatives to T-State Glycogen Phosphorylase *b*[†,‡]

Jennifer L. Martin,[§,∥] Louise N. Johnson,[*] and Stephen G. Withers[⊥]

Laboratory of Molecular Biophysics, The Rex Richards Building, South Parks Road, Oxford OX1 3QU, U.K.

Received May 25, 1990; Revised Manuscript Received July 25, 1990

ABSTRACT: The binding of T-state- and R-state-stabilizing ligands to the catalytic C site of T-state glycogen phosphorylase *b* has been investigated by crystallographic methods to study the interactions made and the conformational changes that occur at the C site. The compounds studied were α-D-glucose, **1**, a T-state-stabilizing inhibitor of the enzyme, and the R-state-stabilizing phosphorylated ligands α-D-glucose 1-phosphate (**2**), 2-deoxy-2-fluoro-α-D-glucose 1-phosphate (**3**), and α-D-glucose 1-methylenephosphonate (**4**). The complexes have been refined, giving crystallographic *R* factors of less than 19%, for data between 8 and 2.3 Å. Analysis of the refined structures shows that the glucosyl portions of the phosphorylated ligands bind in the same orientation as glucose and retain most of the interactions formed between glucose and the enzyme. However, the phosphates of the phosphorylated ligands adopt different conformations in each case; the stability of these conformations have been studied by using computational methods to rationalize the different binding modes. Binding of the phosphorylated ligands is accompanied by movement of C-site residues, most notably a shift of a loop out of the C site and toward the exterior of the protein. The C-site alterations do *not* include movement of Arg569, which has been observed in both the refined complex with 1-deoxy-D-*gluco*-heptulose 2-phosphate (**5**) [Johnson, L. N., et al. (1990) *J. Mol. Biol. 211*, 645–661] and in the R-state enzyme [Barford, D., & Johnson, L. N. (1989) *Nature 340*, 609–616]. Refinement of the ligand complexes has also led to the observation of additional electron density for residues 10–19 at the N-terminus which had not previously been localized in the native structure. The conformation of this stretch of residues is different from that observed in glycogen phosphorylase *a*.

The rapid development of the method of site-directed mutagenesis of enzymes has enabled experimental determination of the contributions that specific atoms or groups of atoms make toward catalysis, binding specificity, and protein stabilization (Fersht et al., 1985, 1986). The complementary approach for protein–ligand interactions compares the binding and kinetic parameters of ligands that differ from each other by relatively small changes in structure (Street et al., 1986). An essential assumption of both approaches is that there is no structural or conformational change in either the ligand or the macromolecule apart from the removal or substitution of the targeted atoms. In this paper, we use the latter method of altering the ligand structure but keeping the macromolecule constant to investigate the binding of related ligands to a protein and to examine the assumption that the protein–ligand complex remains constant when minor changes are made to the structure of the ligand. We compare the refined X-ray crystallographic structures of glycogen phosphorylase complexes with a homologous series of ligands whose kinetic properties are well established.

Glycogen phosphorylase (E.C. 2.4.1.1) is a well-characterized enzyme, present in a wide range of organisms, that catalyzes the phosphorolytic cleavage of α-1,4-linked glucose units to produce α-D-glucose 1-phosphate (Glc-1-P)[1]:

$$\text{glucose}_n + P_i \xrightleftharpoons{\text{phosphorylase}} \text{glucose}_{n-1} + \text{Glc-1-P}$$

The reverse reaction, lengthening of the oligosaccharide by addition of the glucosyl moiety of Glc-1-P to the nonreducing end of the polyglucose chain with concomitant production of phosphate, can be catalyzed in vitro by the enzyme and has been utilized in kinetic experiments whereby phosphate release is taken to be proportional to enzyme activity. The structure, function, regulation, role, and properties of glycogen phosphorylase have been described in a number of reviews (Fischer et al., 1971; Graves & Wang, 1972; Fletterick & Madsen, 1980; Johnson et al., 1989; Newgard et al., 1989).

The activity of mammalian glycogen phosphorylase is controlled by both covalent modification and noncovalent allosteric interactions. Thus, phosphorylase kinase activates the enzyme by covalent addition of a phosphate to a specific serine (Ser14) at the N-terminal tail, resulting in the conversion of phosphorylase *b* (the dephosphorylated enzyme) to phosphorylase *a*. Dephosphorylation is catalyzed principally by phosphatase I. Allosteric control of glycogen phosphorylase may be brought about by a variety of ligands, which can interact with one or more of four different binding sites; these

[†] This work has been supported by the MRC and the SERC. L.N.J. is a member of the Oxford Centre for Molecular Sciences.

[‡] Coordinates of the four refined structures reported in the text have been deposited with the Protein Data Bank, Chemistry Department, Brookhaven National Laboratory, Upton, NY 11973, from which copies are available.

[*] Author to whom correspondence should be addressed.

[§] J.L.M. thanks the Commissioners for the Exhibition of 1851 for financial assistance.

[∥] Present address: Graduate School of Science and Technology, Bond University, Gold Coast, QLD, Australia.

[⊥] Permanent address: Department of Chemistry, University of British Columbia, Vancouver, BC, Canada V6T 1Y6.

[1] Abbreviations: AMP, adenosine 5′-monophosphate; BES, *N*,*N*-bis-[2-hydroxyethyl]-2-aminoethanesulfonic acid; EDTA, ethylenediaminetetraacetic acid; 2-F-Glc-1-P, 2-deoxy-2-fluoro-α-D-glucose 1-phosphate; Glc-1-P, α-D-glucose 1-phosphate; Glc-1-Me-P, α-D-glucose 1-methylenephosphonate; Hept-2-P, 1-deoxy-D-*gluco*-heptulose 2-phosphate; IMP, inosine 5′-monophosphate; PLP, pyridoxal 5′-phosphate; UDPG, uridine(5′)diphospho(1)-α-D-glucose. Sites C, G, N, and I refer to the catalytic, glycogen storage, nucleoside inhibitor, and allosteric effector sites, respectively.

0006-2960/90/0429-10745$02.50/0

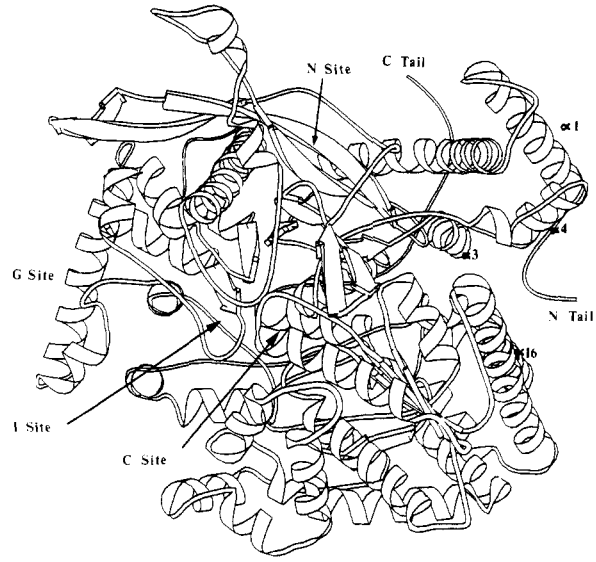

FIGURE 1: Structure of T-state glycogen phosphorylase *b* complexed with glucose (not shown). The positions of the four ligand binding sites and the N- and C-terminal tails are indicated. Helices α1, α3, α4, and α16 are labeled for comparison with Figure 9 [drawn by using RIBBON (Priestle, 1988)].

binding sites are the catalytic or C site, the allosteric activator or N site, the inhibitor or I site, and the glycogen storage or G site. Figure 1 shows the locations of these binding sites on the monomer of glycogen phosphorylase *b*. The C site is situated at the center of the enzyme and contains the essential cofactor pyridoxal phosphate (linked by a Schiff base to Lys680). Access to the C site is blocked by a loop of residues called the 280s loop, which also contributes one of its residues (Phe285) to form part of the I site (located about 12 Å from the C site).

The activation mechanism is associated with a shift in equilibrium from the low-affinity T-state conformation to the high-affinity R-state (Monod et al., 1965) through tertiary and quaternary structural changes promoted by ligand binding (Barford & Johnson, 1989). Glucose is recognized as an inhibitor of phosphorylase *a* that promotes the T-state (Cori & Cori, 19840; Kasvinsky et al., 1978; Sprang et al., 1982), and this inhibition is synergistic with binding of aromatic compounds (AMP, IMP, and caffeine) to the I site. Conversely, AMP and Glc-1-P promote activation of phosphorylase *b* through binding at the N site and the C site, respectively, and favoring the R-state. Thus ligands can be categorized according to whether they promote the T-state or the R-state (Newgard et al., 1989). However, not all R-state-stabilizing compounds are activators of the enzyme, since ligands that bind to the C site and stabilize the R-state may also compete with substrate for binding.

The crystal structures of a number of different forms of the rabbit skeletal muscle enzyme have been solved—T-state phosphorylase *a* (which has glucose bound at the C site; Sprang & Flatterick, 1979), T-state phosphorylase *b* (which has IMP bound at the I site; Sansom et al., 1985; Acharya et al., unpublished work), R-state phosphorylase *b* (which uses sulfate to mimic phosphate at Ser14; Barford & Johnson, 1989), and R-state phosphorylase *a* (Barford, Hu, and Johnson, unpublished work). Comparison of the structures of T-state phosphorylase *a* and *b* (Sprang et al., 1988) has shown the effects of phosphorylation of the N-terminal tail, while the differences in structure between R- and T-state phosphorylase *b* (Barford & Johnson, 1989) have indicated the mechanism by which allosteric effects are communicated between binding

Scheme I: Structures of **1**, Glucose; **2**, Glc-1-P; **3**, 2-F-Glc-1-P; **4**, Glc-1-Me-P; and **5**, Hept-2-P

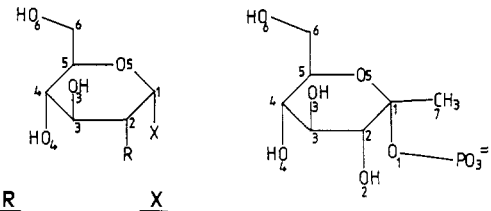

	R	X
1	OH	OH
2	OH	$OPO_3^=$
3	F	$OPO_3^=$
4	OH	$CH_2PO_3^=$

5

sites and between the two subunits of the dimer (the physiologically active form of the enzyme).

In this work we have studied, using crystallographic techniques, the binding of different ligands to the C site of T-state glycogen phosphorylase *b*. The ligands are structurally similar in that they all possess glucosyl moieties, but each has quite different properties. Glucose (Scheme I, compound **1**) stabilizes the T-state of glycogen phosphorylase and exhibits a K_i of 2 mM for inhibition of incorporation of Glc-1-P into glycogen in both phosphorylase *a* and AMP-activated phosphorylase *b* (Sprang et al., 1982). The phosphorylated glucose derivatives represent different classes of R-state-stabilizing ligands. Glc-1-P (**2**), a product (or substrate) of the reversible reaction catalyzed by phosphorylase, has a K_m of 4.8 mM when used as the substrate in the saccharide synthesis reaction catalyzed by AMP-activated phosphorylase *b* (Street et al., 1989). The K_m for Glc-1-P is higher in the T-state compared to the R-state enzyme; Black and Wang (1968) show that, in IMP-activated phosphorylase *b*, Glc-1-P exhibits a K_m of between 32 and 37 mM (depending on the concentration of IMP), while for the AMP-activated enzyme the K_m for Glc-1-P drops to between 4.5 and 9 mM (depending on the concentration of AMP). The dissociation constant, K_d, for Glc-1-P and free phosphorylase *b* is 9.5 mM (Madsen et al., 1976).

2-Deoxy-2-fluoro-α-D-glucose 1-phosphate (2-F-Glc-1-P, **3**) has a K_m of 2.6 mM, and though it can be utilized as a substrate by the enzyme, the rate of reaction is exceedingly slow (over 10^5 times slower than for Glc-1-P). When present in assay medium, it inhibits the utilization of Glc-1-P by AMP-activated phosphorylase *b* with a measured K_i of 2.0 mM (Street et al., 1989). Replacement of the O1 of Glc-1-P by a methylene unit produces α-D-glucose 1-methylenephosphonate (Glc-1-Me-P, **4**), a compound that cannot be used as a substrate but that competitively inhibits the enzyme with a K_i of 0.7 mM (Withers et al., unpublished work).

Although crystallographic binding studies for some of these compounds had been previously carried out (Johnson et al., 1980; Sansom et al., 1983), X-ray measurements were repeated to yield higher resolution and better quality data and to ensure near identical conditions for all four complexes. In addition, crystallographic refinement of each of the ligand complexes has now established the conformational changes in protein and ligand associated with addition or substitution of ligand atoms.

Experimental Procedures

Purified rabbit skeletal muscle glycogen phosphorylase *b* was prepared by the method of Fischer and Krebs (1962) with minor modifications. T-state enzyme was crystallized from the purified protein by using two alternative crystallization media. In the first medium, crystals (Mg type) are obtained from a solution of 20–40 mg/mL glycogen phosphorylase *b*,

2 mM IMP, 10 mM magnesium acetate, 10 mM BES, 0.1 mM EDTA, and 0.02% sodium azide (pH 6.7). In the second medium, crystals (spermine type) were obtained under similar conditions except that the magnesium acetate is replaced by 1 mM spermine and the concentration of IMP is reduced to 1 mM. Both give identical tetragonal crystals with space group $P4_32_12$, unit cell dimensions $a = b = 128.5$ Å and $c = 116.3$ Å, and no detectable changes in structure (Oikonomakos et al., 1985). High-resolution data have been collected previously from both Mg-type (Johnson et al., 1980; Lorek et al., 1984; McLaughlin et al., 1984; Hajdu et al., 1987) and spermine-type crystals (Oikonomakos et al., 1987, 1988). In this work, the availability of crystals resulted in the use of spermine-type crystals (supplied by N. Oikonomakos) in the experiments with glucose and Glc-1-Me-P and Mg-type crystals in experiments with Glc-1-P and 2-F-Glc-1-P.

Prior to data collection, the crystals were soaked in a buffered solution containing the ligand of interest at a concentration of 100 mM. In the experiment with Glc-1-Me-P, 100 mM maltohexaose was also included. Incubation of crystals with Glc-1-P and oligosaccharide results in catalysis and production of phosphate and elongated oligosaccharide chains that eventually disrupt the crystal (Hajdu et al., 1987). Glc-1-Me-P cannot act as a glucosyl donor, so oligosaccharide was added to test whether a pseudoternary enzyme–substrate complex could be observed at the C site. Soak times varied: 1 h for 2-F-Glc-1-P and Glc-1-Me-P, 2 h for Glc-1-P, and 3 h for glucose. The buffer used for spermine-type crystals is composed of 10 mM BES, 0.1 mM EDTA, and 0.02% sodium azide, pH 6.7. For Mg-type crystals, 10 mM magnesium acetate is also included. 2-F-Glc-1-P and Glc-1-Me-P were kindly prepared by Ian Street in one of our laboratories (S.G.W.). All other chemicals were purchased through Sigma Chemical Co.

Data to 2.3 Å were collected on a Nicolet IPC multiwire area detector (Howard et al., 1987) using a Rigaku RU-200 rotating anode X-ray source, with graphite monochromator, operating at 50 kV, 60 mA, and source size 0.3 × 0.3 mm. The detector was placed 16 cm away from the crystal and at a swing angle of 22°. Data frames of 0.2° oscillation were collected with exposure times of 150 s (2-F-Glc-1-P, Glc-1-P, and Glc-1-Me-P) or 200 s (glucose) for a total angular rotation range of at least 90°. The rate of data collection was such that collection time for each of the experiments was always less than 36 h (and for experiments with Glc-1-P and 2-F-Glc-1-P, data collection took less than 24 h). Each experiment was performed with a single crystal of glycogen phosphorylase *b*. The data frames were processed with the XENGEN package of programs (Howard, unpublished work) to produce a scaled set of structure factors. Some measure of radiation damage was assessed by the routine MULTIREF, which determines scales and applies these for intensities from different frames where the frames are grouped in bunches corresponding to 5° of the rotation range. The variation in these scales from start to end of data collection for Glc-1-Me-P (which is typical of other data sets) was 1.07–0.979, indicating a correction corresponding to a 9% fall in intensities. The corrected, scaled, and merged intensities were used as input, along with the native protein structure factors and refined phases (*R* factor 19.1% to 1.9 Å; Acharya et al., unpublished work), to the CCP4 package of crystallographic programs (Daresbury Laboratory, U.K.) for calculation of difference Fourier electron density maps. The initial bound conformations of ligands used in the structure refinement described below were modeled by using these difference Fourier electron density maps.

Structure refinement was performed on a Convex C210 using the molecular dynamics simulated annealing and conventional energy refinement modes of X-PLOR (Brunger, 1988, 1989; Brunger et al., 1989). Simulated annealing involves molecular dynamics simulation of the structure, first at a high temperature to escape local minima and then at room temperature to find a low-energy structure that is consistent with the crystallographic data. The parameters used for the Glc-1-P complex were as follows: high-temperature simulation at 4000 K for 0.5 ps (1000 × 0.5-fs steps) followed by a cooling simulation at 300 K for 1.0 ps (1000 × 1.0-fs steps), with velocity scaling every 25 steps and a tolerance of 0.2 Å. For the glucose and Glc-1-Me-P complexes, the same parameters were used with the exception that the simulation times were reduced (0.3 ps, i.e., 600 × 0.5-ps steps, for both the 4000 K and 300 K simulations). Conventional energy minimization within X-PLOR was performed with a tolerance of 0.05 Å in all cases. For individual atomic *B*-factor refinement, the target standard deviations for bonded atoms and for atoms linked by one other atom were 1.5 and 2, respectively.

The starting structure for the refinement of the Glc-1-P complex included all residues (19–841), but none of the waters, from the refined native protein, plus Glc-1-P modeled into the C site (the structure of Glc-1-P was taken from AM1 energy-minimized coordinates; see below). One round of simulated annealing was performed and then the structure was rebuilt to include residues 16–841. A further round of simulated annealing was performed, after which the structure was again rebuilt to include residues 10–842 and Glc-1-P modeled into the N site. This was then refined by using the conventional least-squares crystallographic energy minimization and *B*-factor refinement of X-PLOR (called energy refinement). Two more rounds of rebuilding and energy refinement were done before waters were added to the structure, and this was followed by seven rounds of rebuilding and energy refinement to give the final refined structure. An obvious conformational change noted at this stage was a displacement on the 280s loop from the C site and a change in 90° in the orientation of Phe285. The starting protein structures for X-PLOR refinement of the glucose and Glc-1-Ne-P complexes were taken from the X-PLOR-refined Glc-1-P complex at the stage before addition of waters (i.e., residues 10–842, *R* factor 20.8%). For the glucose complex, the structure of glucose (Brown & Levy, 1979) modeled into the C site was included in the refinement. For the Glc-1-Me-P complex, Glc-1-Me-P (coordinates from AM1 energy minimization) modeled into both C and N sites and maltopentaose modeled into the G site [coordinates from Johnson et al. (1990)] were also included. The refinement strategy for both the glucose and Glc-1-Me-P complexes was the same—one round of simulated annealing followed by rebuilding, one round of energy refinement followed by addition of waters, and then three more cycles of rebuilding and energy refinement. For the glucose complex, residues 10 and 11 were removed from the structure prior to the last cycle of refinement. The refinement of the glucose complex resulted in a shift of the 280s loop and the Phe285 side chain from their positions in the Glc-1-P complex to positions similar to those of the native uncomplexed structure. The Glc-1-Me-P complex refinement resulted in a similar conformation of the 280s loop to the Glc-1-P refinement but with a slightly greater displacement of the 280s loop away from the catalytic site. These shifts show a pattern of one structure characteristic of the T-state structure (native and glucose complexed) and another characteristic of complexes with R-state ligands (Glc-1-P and Glc-1-Me-P complexes). The structure of the 2-F-Glc-1-P

Table I: Statistics of Data Collection, Processing, and Refinement

ligand	Glc-1-P	glucose	Glc-1-Me-P	2-F-Glc-1-P
crystal size (mm)	4.0 × 0.6 × 0.4	1.6 × 0.4 × 0.4	2.4 × 0.5 × 0.5	2.8 × 1.2 × 0.8
no. of measured reflections	89325	85168	110427	84187
no. of unique reflections	37461	34771	35243	37772
completeness of data[a] (%)	88	82	83	88
$\langle I/\sigma I \rangle$	14.2	18.5	13.8	19.3
$R_m(I)$[b] (%)	6.6	6.9	8.7	5.0
R_{iso}[c] (%)	17.2	11.1	19.3	15.7
initial R factor[d] (%)	28.5[e]	25.7[e]	25.2[e]	25.8[e]
no. of atoms in final cycle of refinement	7430	7361	7478	7428
no. of water molecules in final cycle	605	576	596	605
no. of reflcns used in refinement (8–2.2 Å, $I > 0$)	27612	29460	28429	26600
R factor[d] (%)	18.1	18.1	18.6	18.0
rms dev in bond lengths[f] (Å)	0.017	0.016	0.016	0.016
rms dev in bond angles[g] (deg)	3.5	3.4	3.5	3.5

[a] Number of unique reflections as a percentage of the number predicted to 2.3 Å. [b] Merging R factor for symmetry-related reflections, $R_m = \sum_i\sum_h[|I(h) - I_i(h)|]\sum_i\sum_h[I_i(h)]$, where $I_i(h)$ is the ith intensity measurement of reflection h and $I(h)$ is the mean intensity for that reflection. [c] Mean fractional isomorphous difference of the structure factor amplitudes of the ligand protein complex (F_L), calculated with respect to the structure factor amplitudes of the native enzyme (F_p): $\sum_h[||F_L| - |F_P||]/\sum_h|F_P|]$. [d] Crystallographic R factor, $\sum||F_o| - |F_c||/\sum|F_o|$, where $|F_o|$ and $|F_c|$ are the observed and calculated structure factor amplitudes, respectively. [e] See Experimental Procedures for starting conformations. [f] rms deviation from ideal bond lengths. [g] rms deviation from ideal bond angles.

complex was refined by the simple method of taking the final refined structure of the Glc-1-P complex, replacing with fluorine the O2 hydroxyl of Glc-1-P, at both C and N sites, and performing energy refinement on this structure, first without waters and then with waters added. X-PLOR parameters for nonprotein atoms (Martin, 1989) are available from the authors. These have been derived from parameters for similar ligands available with the X-PLOR package (e.g., carbohydrate parameters from Weiss, unpublished work, were modified to produce the phosphorylated glucose parameters) and are similar to those described by Johnson et al. (1990).

$2F_o - F_c$ electron density maps were generated from X-PLOR-refined coordinates by using the CCP4 package of programs. Maps and structures were displayed, and rebuilding was performed, with the molecular graphics program FRODO (Jones, 1975, 1978; modified by J. W. Pflugrath, M. Saper, R. Hubbard, and P. Evans) implemented on an Evans and Sutherland PS300 or PS390 graphics terminal on-line to a VAX 6210. Hydrogen bonds were assigned by FRODO if the distance between two electronegative atoms was less than 3.3 Å and if both angles between these two atoms and each of the preceding atoms are greater than 90°. Van der Waals interactions were assumed where non-hydrogen atoms are separated by less than 4 Å. Protein structural changes were measured by using the programs ASH (Hendrickson, 1979; D. I. Stuart, unpublished work) and DEVIAT (A. Martin, unpublished work) with the native protein (residues 10–842) refined by X-PLOR (R factor 21% for all reflections between 8 and 1.9 Å; Acharya et al., unpublished work).

Conformational energy calculations on small molecules were performed with the AM1 Hamiltonian (Dewar et al., 1985) of the semiempirical molecular orbital package AMPAC/MOPAC (QCPE No. 506). For the AM1 calculations on the phosphorylated ligands, the phosphate group was assumed to be a dianion. In all cases, rotation of the hydrogen attached to O4 was restricted to prevent formation of a hydrogen bond to the phosphate, which requires a distorted ring conformation. Program GRID (Goodford, 1985; Boobbyer et al., 1989) was used to predict the interaction energy for a phosphate probe group at the C site of glycogen phosphorylase.

Results

The statistics for data collection and refinement are given in Table I. The data collection strategy resulted in data sets that are at least 82% complete with the fraction of intensities between 2.32 and 2.47 Å about 45% complete. The crystallographic data (R_m between 5% and 8.7%) and the final refined structures (crystallographic R factors all less than 19%, with reasonable stereochemistry) are satisfactory.

Difference Fouriers. In all four experiments, the highest peak in the difference Fourier occurs at the C site, corresponding to the binding of the glucosyl ligand. For the glucose complex, no other changes were indicated except displacement of a water molecule by O3 of the glucosyl ring and movement of His377 to accommodate the O6 hydroxyl; both of these changes have been observed in other experiments where glucose-like structures are bound to the catalytic site (Oikonomakos et al., 1988). These features are also apparent in the difference Fouriers of the phosphorylated glucose derivatives, but with these ligands other changes are also observed: (1) there is negative density over residues Asp283 and Asn284 and much of the rest of the 280s loop and over some of the residues 375–378, which interact with the 280s loop; (2) there is negative and positive electron density near the imidazole ring of His571, which makes a hydrogen bond to Asp283 in the native structure, indicating rotation of the ring; (3) there is negative density that envelopes the whole side chain of Arg569, but there is no positive density in which to build a new conformation; an (4) there is negative density over Tyr613 and Phe285, which indicates disruption of the inhibitor binding I site. Similar difference Fourier maps have been observed for other R-state-stabilizing complexes, such as those with UDPG (Oikonomakos et al., 1988) and with Hept-2-P (McLaughlin et al., 1984), except that in the case of Hept-2-P there is strong positive density indicating the new conformation of Arg569.

For the phosphorylated ligands Glc-1-P, Glc-1-Me-P, and 2-F-Glc-1-P, there is density at the N site indicative of binding of the ligands there, and for the Glc-1-Me-P complex there is strong positive density at the G site for maltohexaose (but no indication that the oligosaccharide binds at the catalytic site).

X-PLOR-*Refined Structures.* The refined structures agree very well with electron density maps calculated by using the $2F_o - F_c$ coefficient (e.g., Figure 2 for Glc-1-P at the C site), even for the Glc-1-Me-P complex, where the difference Fourier was rather noisy. Comparison of the refined Glc-1-P, 2-F-Glc-1-P, and Glc-1-Me-P complexes with the X-PLOR-refined native enzyme showed essentially identical changes. Figure 3 (for the Glc-1-Me-P complex) shows that the regions where

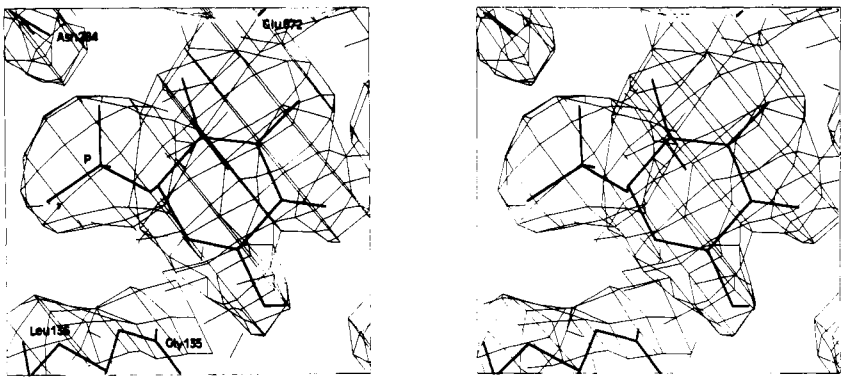

FIGURE 2: Stereo diagram of the C site of the refined Glc-1-P complex showing the bound conformation of Glc-1-P (phosphate group labeled P) and electron density from the $2F_o - F_c$ map.

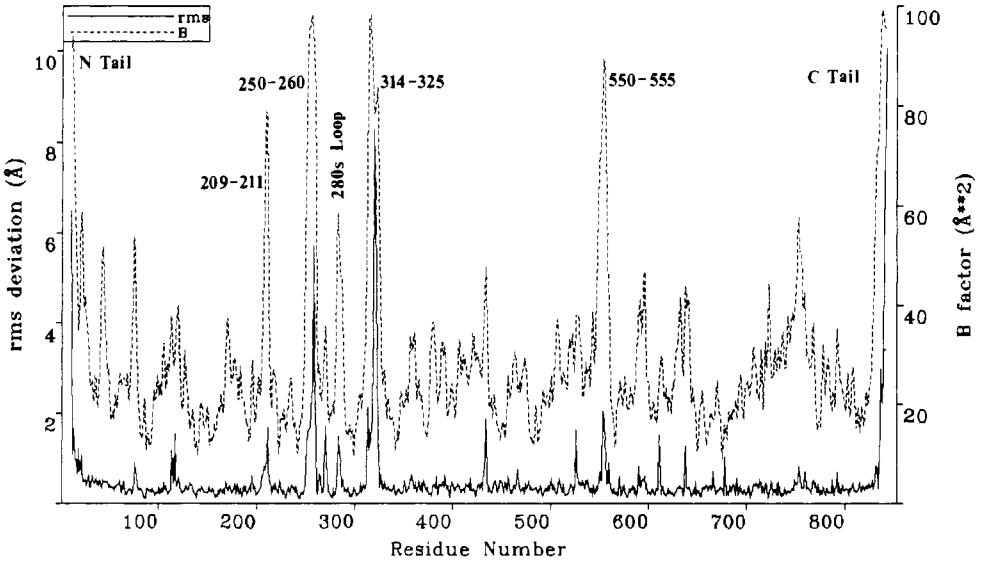

FIGURE 3: Plot per residue of the rms deviation (Å) (continuous line) between the atoms of the refined Glc-1-Me-P complex and the native enzyme (Acharya et al., unpublished work) and of the average B factors (Å^2) (dashed line) of the Glc-1-Me-P complex. Regions with high rms deviation and B factors greater than 60 Å^2 are labeled. These correspond to similar flexible regions in the native protein (Acharya et al., unpublished work) except for the 280s loop, which has low B factors in the native structure and in the glucose-bound complex.

the greatest changes in structure occur are those that are known to be flexible (Sprang et al., 1988; Acharya et al., unpublished work), such as the loop regions, 250–260 and 314–325, and the C-terminus; these regions have little associated electron density and very high temperature factors. In addition, the rms deviation for the 280s loop (which is well ordered and has low B factors in the native structure) is over 1 Å, and the average B factors are very high. The implied structural alteration is consistent with the observation from the difference Fourier. The rms differences for the glucose complex are similar to those shown in Figure 3 except that the movement of the 280s loop is not observed. The overall rms difference for backbone atoms of the complexes compared to the native enzyme (excluding the very poorly defined regions 250–260, 314–325, and the C-terminus residues 838–842) are as follows: glucose, 0.42 Å, Glc-1-P, 0.40 Å, 2-F-Glc-1-P, 0.41 Å, and Glc-1-Me-P, 0.46 Å.

Interactions between the Glucosyl Moieties and the C Site. A list of the hydrogen-bond contacts formed between the ligands and the C site is given in Table II. Van der Waals contacts are also made to Gly134, Leu139, Val455, and Thr676. The interactions formed by the glucosyl portions of 2-F-Glc-1-P, Glc-1-P, and Glc-1-Me-P to the C site are essentially the same as those to glucose with phosphorylase *b* (including the displacement of a water molecule by the O3 hydroxyl) and those described for the interactions of glucose with phosphorylase *a* (Sprang et al., 1982; Street et al., 1986). However, because of movement of the 280s loop when the phosphorylated ligands bind (see also next section), the hydrogen bond formed between Asn284 and the O2 hydroxyl of glucose is no longer found in the phosphorylated glucose complexes. Similarly, a slight displacement, compared with glucose, of each of the phosphorylated ligands away from Asn484 lengthens or removes the hydrogen bond formed between that residue and the O4 hydroxyl. A hydrogen bond to O1 of glucose from a water molecule, OH8 872, is not present in the other complexes because the water is displaced by the phosphate group; another water, OH7 910, is also displaced by the phosphorylated glucose derivatives but not by glucose, though no hydrogen bond is formed between OH7 910 and glucose. The rms deviation for the glucosyl atoms of the phosphorylated ligands compared with those of glucose is 0.34 Å for Glc-1-P and 0.30 Å for Glc-1-Me-P but 0.5 Å for 2-F-Glc-1-P. This larger difference for 2-F-Glc-P is probably a result of an unfavorable ionic interaction between F2 and Glu672 that forces the glucosyl moiety away from the acidic residue, while in the other complexes a hydrogen bond is predicted between the O2 hydroxyl and Glu672. Figure 4 shows a superimposition of the bound conformations of the ligands in which the displacement of 2-F-Glc-1-P away from Glu672 is evident.

Interactions between the Phosphate Moieties and the C Site. Figure 4 also illustrates the most striking feature of the bound phosphorylated ligand structures, that is, the difference in

Table II: Hydrogen-Bond Contacts[a] between Glucosyl Ligands and Residues of the C Site of Glycogen Phosphorylase *b*

ligand atom	protein atom	glucose	2-F-Glc-1-P	Glc-1-P	Glc-1-Me-P
O1	WAT OH8 872	3.0			
O2[b]	ND2 Asn284	3.2			
	OH Tyr573		2.9		3.2
	OE1 Glu672	2.9	3.3	3.1	2.9
	WAT OH7 890	3.0	3.2	2.5	2.9
O3	OE1 Glu672	2.9	2.9	2.7	3.0
	N Ala673	(3.4)	3.1	3.3	(3.4)
	N Ser674	3.0	3.1	3.0	3.0
	N Gly675	3.0	3.3	2.9	2.8
O4	OD1 Asn484	3.1			3.2
	N Gly675	2.8	2.7	2.6	2.8
	WAT OH1 897	2.6	2.7	2.8	2.9
O5	ND1 His377			3.0	
O6	ND1 His377	2.7	2.7	2.6	2.6
	OD1 Asn484	3.0	3.0	2.9	3.2
O7	N Gly135		2.8	2.6	2.7
O8	N Gly135		3.0	3.3	
	N Leu136		2.8		
	ND2 Asn284				2.5
	WAT OH0 887		3.0	3.2	
O9	ND2 Asn284		2.6	2.6	
	NZ Lys574				2.5
	OP2 PLP[c]		4.5	3.7	3.3
	O2 ligand[d]		(3.4)	3.0	3.3

[a] Distances are listed in angstroms for those hydrogen bonds found in the C site of the ligand–enzyme complexes in the X-PLOR-refined structures by using the hydrogen-bond search routine implemented in FRODO (P. Evans, unpublished work). This method predicts hydrogen bonds where the separation of the two hydrogen bonding atoms is less than 3.3 Å and where the two angles made by these atoms and the adjacent covalently bonded atoms are both greater than 90°. [b] For 2-F-Glc-1-P, distances are measured to F2. [c] Distance to phosphate oxygen of cofactor pyridoxal phosphate. [d] Intramolecular distance to glucosyl O2 hydroxyl (or F2 in the case of 2-F-Glc-1-P).

conformation of the phosphate groups. The phosphate dihedral angle (ϕ, O5–C1–O1–P for Glc-1-P and 2-F-Glc-1-P and O5–C1–C7–P for Glc-1-Me-P) is 114° for 2-F-Glc-1-P, 152° for Glc-1-P, and 180° for Glc-1-Me-P. The transition state analogue Hept-2-P (**5**) binds to the catalytic site with a ϕ value of 224° (Johnson et al., 1990). On going from the 2-F-Glc-1-P conformation to the Hept-2-P conformation, the phosphate successively moves closer to the cofactor phosphate; the P–P distance is 6.9 Å for 2-F-Glc-1-P, 6.1 Å for Glc-1-P, 5.5 Å for Glc-1-Me-P, and 4.8 Å for Hept-2-P. For Glc-1-Me-P (where data was collected from a crystal soaked in a solution containing both Glc-1-Me-P and maltohexaose) and Hept-2-P, the phosphate oxygens are sufficiently close to the PLP phosphate to allow hydrogen-bond formation. This variety of phosphate binding conformations gives rise to a number of different interactions between the phosphate and the protein (Table II). The common interactions for the three ligand phosphates are a hydrogen bond/helix dipole interaction with Gly135 and a hydrogen bond to Asn284. For the Glc-1-Me-P phosphate there is also a short hydrogen/ionic bond with Lys574. An intramolecular hydrogen bond from the phosphate oxygen to the O2 hydroxyl is present in both Glc-1-P and Glc-1-Me-P but not in 2-F-Glc-1-P. Presumably the O2 hydroxyl acts as a proton donor, and this is not possible on replacement by fluorine at the 2 position. The phosphate of Hept-2-P makes different interactions from those described here (Johnson et al., 1990), in particular two ionic bonds to Arg569; these are possible for the Hept-2-P complex since Arg569 moves from its buried position to interact with the Hept-2-P phosphate. In the structures reported here, the refined position of Arg569 is buried and thus inaccessible for interaction with the ligand phosphates.

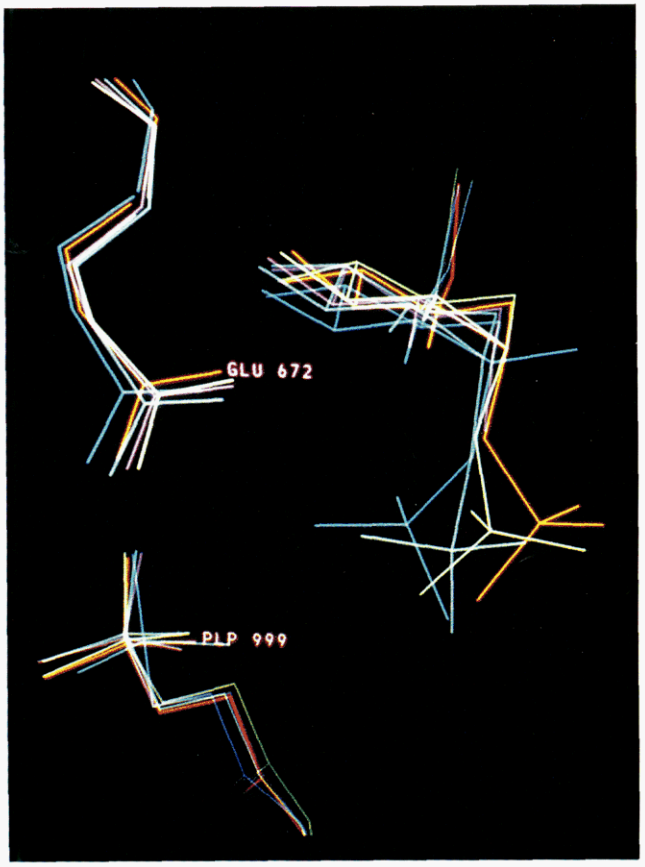

FIGURE 4: Superimposition of the refined bound conformations of glucose (purple), 2-F-Glc-1-P (orange), Glc-1-P (light green), Glc-1-Me-P (light blue), and Hept-2-P (dark blue) (Johnson et al., 1990). The C-site residue Glu672 and the PLP cofactor from the five refined structures are also shown.

An interesting result of the refinements is that in all of the phosphorylated ligands the bond angle C1–O1–P (or C1–C7–P in the case of Glc-1-Me-P) is distorted. For 2-F-Glc-1-P and Glc-1-P, the optimal value for this angle is 120° but the refined values are both 129°. Likewise, for Glc-1-Me-P the final refined value is 128° though the preferred angle is 110°. Given that the rms deviation in bond angles is about $3^1/_2$° for all of these structures, this distortion is significant. The same angle for the refined structure of Hept-2-P is 135° (ideal value 120°).

Stability of Alternative Ligand Phosphate Conformations. The question of why the phosphorylated ligands bind to the enzyme with different phosphate conformations presents an intriguing puzzle. The bound Glc-1-P conformation observed here represents the conformation recognized by the T-state enzyme in which only two hydrogen bonds are made by the phosphate oxygens to the protein, compared with six hydrogen bonds made by the transition-state analogue Hept-2-P. The phosphate conformation (see Figure 5a) may be influenced by a number of factors, including the following.

(*a*) *Internal Steric Effects.* The position of the phosphate group relative to the glucopyranose ring is measured by the torsion angle ϕ (O5–C1–O1–P, or O5–C1–C7–P in the case of Glc-1-Me-P) and the bond angles at C1 and O1. For ϕ values between 240° and 360° (0°), the phosphate is placed under the glucosyl ring or eclipsed with respect to the C1–O5 (0°) or C1–C2 (240°) bonds, and so these conformations are sterically unfavorable, but conformations between 0° and 240° should be accessible. For Hept-2-P, the presence of the β-methyl group at C1 should destabilize the 120° conformation (phosphate eclipsed with respect to β-methyl) because of un-

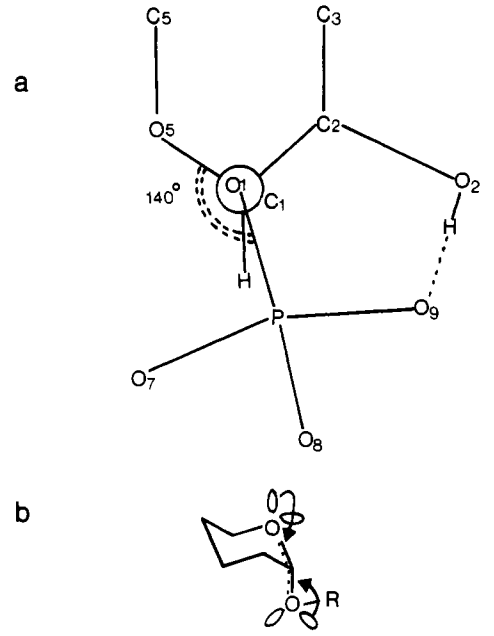

FIGURE 5: (a) Projection looking down the O1–C1 bond of Glc-1-P (not drawn to scale). The dihedral angle ϕ (O5–C1–O1–P) of the phosphate in this diagram is 140°, at which conformation a hydrogen bond between the phosphate oxygen and the O2 hydroxyl may occur. At 0°, the O1–P bond is eclipsed with the C1–O5 bond. At 120°, the O1–P bond is eclipsed with the C1–H bond, and at 240°, it is eclipsed with the C1–C2 bond. Dihedral angles between 240° and 360° (0°) place the phosphate under the glucosyl ring, which is sterically unfavorable. (b) Schematic diagram showing the anomeric effect, delocalization of O5 and O1 lone pair orbitals, in α-glycosides. For α-glycosides, the lone pair orbital of O5 is always antiperiplanar to the C1–O1 bond, but the O1 (exo anomeric) delocalization depends upon rotation around the C1–O1 bond.

favorable steric interactions between the phosphate and the β-methyl group.

(*b*) *The Anomeric Effect.* A stereoelectronic conformational preference is exerted when two electronegative atoms are separated by an electron-deficient atom (Kirby, 1983); e.g., the O5–C1–O1 group of these sugars. The general anomeric effect occurs when a lone pair orbital of one of the electronegative atoms is disposed antiperiplanar (180°) to the C–O bond of the other electronegative atom, resulting in charge delocalization of the lone pair electrons, which is observed as a shortening of the O–C bond (Fuchs et al., 1984). Figure 5b illustrates the two possible sources of the anomeric effect in α-glycosides: (1) charge delocalization about the fixed bond of O5 (the endo anomeric effect) and (2) the charge delocalization that can occur about O1 at certain ϕ values where the lone pair orbitals are antiperiplanar to O5 (the exo anomeric effect). The small molecule crystal structures of α-D-glucose 1-phosphate (Narendra & Viswamitra, 1984; Narendra et al., 1984; Suguwara & Iwasaki, 1984) have the phosphate at the exo anomeric stabilized gauche$^+$ conformation (ϕ of 90°), and the bond lengths of both O5–C1 (1.42 Å) and C1–O1 (1.40 Å) are short, consistent with both endo and exo anomeric effects. Rotation of the phosphate to ϕ values between 60° and 90° is calculated to stabilize α-glycosides by 3–4 kcal/mol compared with other phosphate conformations (Fuchs et al., 1984). Exo anomeric stabilization of ϕ values between 60° and 90° may be important in Glc-1-P, 2-F-Glc-1-P, and Hept-2-P but should not affect Glc-1-Me-P where, of course, there are no O1 lone pair orbitals.

(*c*) *Effect of the Enzyme.* The enzyme can impose steric restrictions on the conformational freedom of the glucosyl phosphate, or it may stabilize unfavorable conformations by formation of hydrogen bonds or ion pairs. Examination of the enzyme structure indicated that conformations of the phosphate group between 0° and 100°, that is, including the exo anomeric stabilized conformations, would be sterically hindered by protein residues Gly135 and Leu136. The conformations available to the phosphorylated ligands *in the enzyme* are thus restricted to the range 110°–240° (the conformations of the bound glucosyl phosphates all fall within this range).

Table III: Relative Energies[a] (kcal/mol) of Different Phosphate Conformations for Phosphorylated Glucose Derivatives

ϕ conformation (O5–C1–O1/ C7–P)	2-F-Glc-1-P (minimum at 79°)	Glc-1-P (minimum at 135°)	Glc-1-Me-P (minimum at 144°)	Hept-2-P (minimum at 186°)
110°	0.8[b]	3.1	7.0	3.0
120°	1.1	0.9	3.3	0.9
140°	2.6	0.1	0.2	0.1
150°	3.4	0.8[b]	0.2	0.4
180°	4.0	3.0	3.2[b]	0.2
200°	5.4	4.4	4.1	0.9
220°	5.9	5.0	4.6	2.4[b]

[a] Each of the conformations has been optimized by using AM1 (see Experimental Procedures) and the energy then compared to the lowest energy conformation—the global minimum—to give the relative energy for that conformation (the global minimum conformation is given a relative energy of 0 kcal/mol). [b] Conformation closest to that observed bound in the crystal structure of the glycogen phosphorylase *b*–ligand complex.

(*d*) *Electrostatics and Hydrogen Bond Formation.* ϕ values between 140° and 220° might be energetically favored because of the possibility of formation of an internal hydrogen bond between the phosphate and the O2 hydroxyl.

To try to understand the effects that contribute to the final bound conformation of the ligands, in vacuo AM1 conformational energy calculations were performed (i.e., the effect of the enzyme was not included). Minimum energy conformations and the relative energies of different conformations of the ligands (including Hept-2-P) are given in Table III.

For 2-F-Glc-1-P, where there is no possibility of forming a stabilizing hydrogen bond between the phosphate and the O2 hydroxyl (because it has been replaced by fluorine), the in vacuo calculated lowest energy conformation is the exo anomeric stabilized ϕ = 79°. This conformation is prohibited in the enzyme because of steric clashes, and the enzyme-bound conformation has the phosphate at 114° (as far away from the 2-fluoro group as allowed, given the restraints of the C site). The calculated energy of the phosphate at 110° is 0.8 kcal/mol, and this is the lowest energy of 2-F-Glc-1-P within the range of C-site permitted conformations. As the phosphate is rotated from 110° to 220°, and so moves closer to the 2-fluoro group, the energy of the system steadily increases to 5.9 kcal/mol.

The calculated minimum energy conformation of Glc-1-P is 135°, and the bound conformation (152°, 0.8 kcal/mol) of Glc-1-P is reasonably close to this. This conformation is sterically favorable, both in vacuo and in the enzyme, *and* it is stabilized by a hydrogen bond between the phosphate and the O2 hydroxyl. For Glc-1-P there is a very narrow range of conformations within 1 kcal/mol of the global minimum, the range being from 120° to 160°.

In the case of Glc-1-Me-P, which is not affected by the exo anomeric effect because O1 is replaced with a methylene group, the lowest energy conformation is 144°, similar to that calculated for Glc-1-P. However, the observed bound conformation in the enzyme has a dihedral angle of 180°, which is some 3 kcal/mol higher than the minimum energy conformation. At this conformation a hydrogen bond is formed between the phosphate and the O2 hydroxyl (in both the

calculated and observed bound structures), but as in all the complexes, this intramolecular hydrogen bond may be formed at the expense of, or is possibly shared with, a hydrogen bond donated by O2 to Glu672.

For Hept-2-P the calculated lowest energy conformation is at 186°. In contrast to Glc-1-P and Glc-1-Me-P, the range of conformations within 1 kcal/mol of this global minimum is quite broad, from 120° to 200°. This shallow potential energy well for Hept-2-P is a result of the β-methyl group at C1, which destabilizes (compared with Glc-1-P) the phosphate at dihedral angles between 120° and 150°. So, for Hept-2-P the conformations around 140° are just as favorable as the conformations around 180°. The difference in energy between the calculated global minimum and the bound (220°) conformation of Hept-2-P is 2.4 kcal/mol, which is half that calculated for Glc-1-P to achieve the 220° conformation (5 kcal/mol).

Conformational Changes at the C Site. There is very little change in the structure of glycogen phosphorylase *b* on binding glucose. This observation is consistent with previous results, which suggest that this crystal form of the enzyme is the T-state conformation (Sprang et al., 1988) and that glucose stabilizes the T-state of the enzyme (Kasvinsky et al., 1978, 1981). While the T-state C site is able to accommodate glucose without significant changes in structure, it cannot accept the additional bulk of a phosphate attached to glucose at C1. Figure 6a shows the size of the C site with contours drawn by GRID for a phosphate probe in the T-state glucose-bound phosphorylase *b*. For clarity, the enzyme residues are not shown, but the position of bound Glc-1-P is superimposed on the map to show that the phosphate moiety extends outside the contours that delineate the boundaries of the C site in the T-state enzyme. Obviously, some alteration in C-site structure is necessary to allow phosphorylated glucose derivatives to bind. An increase in C-site size does occur on binding the phosphorylated ligands, as illustrated in Figure 6b, which is an analogous plot to that of Figure 6a but shows the phosphate-accessible regions of the C site for the Glc-1-P complex. Once again, Glc-1-P has been superimposed in its refined bound conformation. The comparison of panels a and b in Figure 6 shows quite clearly the increase in size of the C site. A similar increase occurs in the complexes with 2-F-Glc-1-P and Glc-1-Me-P.

Most of the increase in cavity size on going from glucose-bound to phosphorylated ligand bound enzymes is a result of movement of the 280s loop, which is pushed out of the C site (Figure 7a) along the channel 1 pathway (Barford et al., 1988). Other changes in enzyme conformation that contribute to an increase in the size of the C site include the movement of His377 to make room for the O6 hydroxyl of the glucose portion of the ligands (this also occurs in the glucose-bound enzyme) and rotation of His571, which makes a hydrogen-bond contact with Asp283 in the native and glucose-bound structures; it rotates around the CB–CG bond to make a new hydrogen bond with Tyr613 in the Glc-1-P bound enzyme or to form a hydrogen bond to Asp283 (in its new position) in the Glc-1-Me-P and 2-F-Glc-1-P complexes. Two water molecules are also displaced by the ligand phosphates (see previous section).

A further indication of the magnitude of the changes in structure that occur at the C site when these ligands bind is given in Table IV, which compares the refined ligand bound structures with the native structure in two ways: (i) rms deviation in positions of all atoms constituting the C site, and (ii) temperature (*B*) factors of residues that constitute the C site. The numbers reiterate that when glucose binds, there is only a very small change in structure; the *B* factors of all residues and the ligand are as low as those of the native. However, for Glc-1-P, 2-F-Glc-1-P, and Glc-1-Me-P bound structures there is a more substantial change in C site structure, and the *B* factors of the ligands and many residues (especially the 280s loop) are higher than for the native and glucose-bound enzymes.

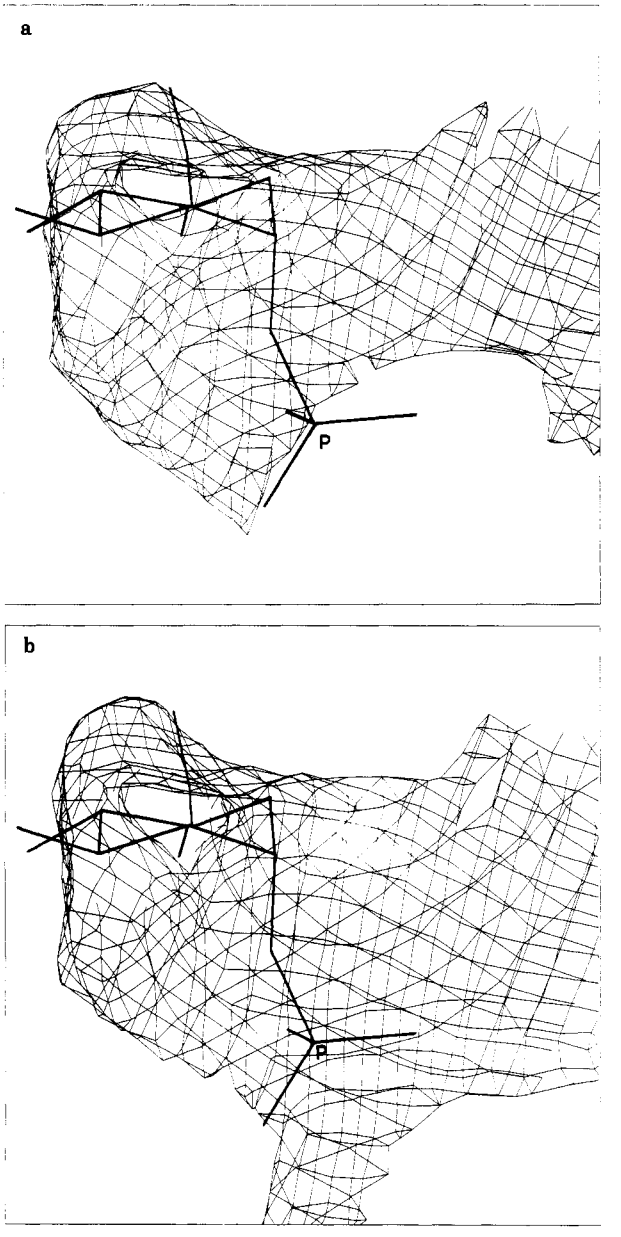

FIGURE 6: GRID predicted contours of the interaction energy (including Lennard–Jones, hydrogen bonding, and ionic energy) of a spherical probe group, in this case phosphate, at each point on a three-dimensional grid (of spacing 0.33 Å) at the C site of (a) the glucose-bound and (b) the Glc-1-P bound enzymes. Contours corresponding to a slightly unfavorable energy (0.5 kcal/mol) are shown to indicate the size and shape limits of the cavity at the C site. The refined conformation of Glc-1-P is superimposed upon the contours to show that the phosphate group (labeled P) does not fit within the available space in the glucose-bound enzyme but that the larger cavity in the Glc-1-P bound enzyme does accommodate the phosphate. Note that some of the hydroxyl groups protrude through the phosphate probe contours, though they do not protrude through contours defined by using a smaller hydroxyl probe (not shown), which accesses more of the C site than the phosphate probe.

Conformational Changes at the I Site. Movement of the 280s loop on binding of phosphorylated ligands at the C site

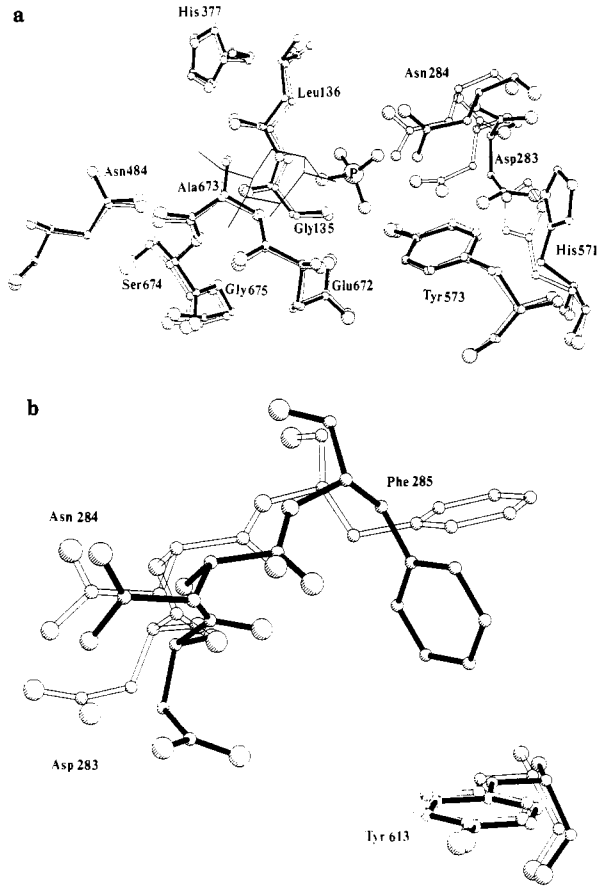

FIGURE 7: (a) Superimposition of C-site residues from the glucose (light bonds) and 2-F-Glc-1-P (dark bonds) enzyme complexes. For clarity, the structure of glucose is not shown and the glucosyl part of 2-F-Glc-1-P is drawn as a single line. The phosphate of 2-F-Glc-1-P (labeled P) is drawn with thicker bonds and spheres for atoms. Most of the protein residues remain unchanged whether glucose or the phosphorylated glucose derivatives bind at the C site. However, as shown here for the 2-F-Glc-1-P complex, the phosphorylated glucose derivatives induce movement of Asp283, Asn284, and His571. (b) Superimposition at the I site of Tyr613 and the 280s loop residues Asp283, Asn284, and Phe285 from the complexes of phosphorylase with glucose (light bonds) and with 2-F-Glc-1-P (dark bonds). In this view, the C site is situated to the left of Asp283 and Asn284. I-site inhibitors intercalate between Phe285 and Tyr613 when they are stacked parallel to each other (e.g., glucose-bound enzyme); movement of Phe285 to a position where the phenyl ring is perpendicular to Tyr613 (as occurs in the refined complexes with 2-F-Glc-1-P, Glc-1-P, and Glc-1-Me-P) would prevent inhibitors from binding at the I site (PLUTO; S. Motherwell, unpublished results).

has repercussions at the I site, which is formed in part by residues of this loop. In the native and glucose-bound structures Phe285 stacks in an approximately planar orientation, some 7 Å away from Tyr613. When the phosphorylated ligands bind at the C site, the induced 280s loop motion causes Phe285 to slide past Tyr613 and the final interaction is perpendicular (Figure 7b). However, the electron density for Phe285 from the $2F_o - F_c$ maps for the Glc-1-P, 2-F-Glc-1-P, and Glc-1-Me-P complexes is rather diffuse, implying that a number of different conformations may be available to this side chain. The conformational changes and the increase in average *B* factor of the 280s loop indicate destabilization of the inhibitor binding I site, induced by the binding of R-state-stabilizing ligands at the C site.

N Site. For the Glc-1-P, 2-F-Glc-1-P, and Glc-1-Me-P complexes, refinement included the phosphorylated ligands bound at the N site. In all these cases the density for the phosphate portion of the bound ligands is much stronger than for the glucosyl part of the structure, and all but one (Arg193 interaction with the glucosyl O5 or O6) of a total of seven hydrogen-bond contacts to the ligand are formed to the phosphate (Arg242 makes one hydrogen bond, Arg309 three, and Arg310 two). The lack of specific interactions to the glucosyl ring and the poor density for the glucosyl portion of the ligand indicate that the important factor for binding at this site is the presence of the phosphate. The average *B* factors for the ligands bound at the N site are high, 60–70 Å^2.

Table IV: Comparison of the C Site of Native and Ligand-Bound Phosphorylase *b*

	phosphorylase complex				
	native	glucose	Glc-1-P	Glc-1-Me-P	2-F-Glc-1-P
rms dev of catalytic site[a] (Å)		0.64	0.92	1.04	0.98
average *B* factor (Å^2)					
protein atoms (N, C, O, Cα, Cβ)	25	24	32	29	32
ligand		15	39	35	35
281–286	26	18	56	49	63
376–384	22	19	34	30	35
Arg569	19	18	31	32	34
Tyr613	22	19	33	26	31
671–676	15	11	22	17	20
PLP	11	11	17	12	16

[a] rms deviation (calculated with DEVIAT; A. Martin, unpublished work) compared with the native structure, including all atoms of residues 88, 132–137, 281–286, 376–384, 568–574, 613, and 671–676 and of PLP.

G Site. In the $2F_o - F_c$ map of the Glc-1-Me-P complex, there is strong electron density for five glucose units at the major binding site and weak density for one glucose unit at the minor binding site of the G site. The glucose units at the major binding site were modeled in the X-PLOR refinement. The bound conformation of the oligosaccharide and the interactions it makes with the enzyme have been described in detail elsewhere (Sansom, 1983; Barford, 1988; Johnson et al., 1990) and will not be discussed further except to mention that interactions are formed predominantly to S4 and S5 of the oligosaccharide, that this involves contacts to residues Asn407, Ser429, Glu433, and Lys437, and that the average *B* factors of each of the glucosyl units are similar to those given in Johnson et al. (1990).

N-Terminus. During refinement of the Glc-1-P complex, additional electron density was observed at the N-terminus into which residues 10 to 18—previously assumed to be disordered or mobile—were modeled. This stretch of residues was also incorporated into the refinement of the other three complexes, and the resulting conformations and positions of residues from Ile13 is very similar. However, in all of the final refined structures the position of Arg10, Lys11, and Gln12 is still uncertain; the electron density for these residues is poor, and the temperature factors are over 100 Å^2. Indeed, for the glucose complex, Arg10 and Lys11 were excluded from the final cycle of refinement because of the very high *B* factors (around 150 Å^2) and the paucity of density in which to place the residues. Electron density for the rest of the N-terminal tail is satisfactory (e.g., Figure 8) and the *B* factors are reasonable, averaging around 60 Å^2, compared with average *B* factors of over 90 Å^2 for the flexible loop regions 250–260 and 314–325. The native enzyme has been refined with the additional N-terminal residues by using X-PLOR (Acharya et al., unpublished work), and the final conformation and position of the tail is similar to that described here, though the *B* factors of this region in the native structure are higher.

The N-terminal tail is in an extended β-strand conformation with a bend, or hydrogen-bonded turn, at Val15. The extended

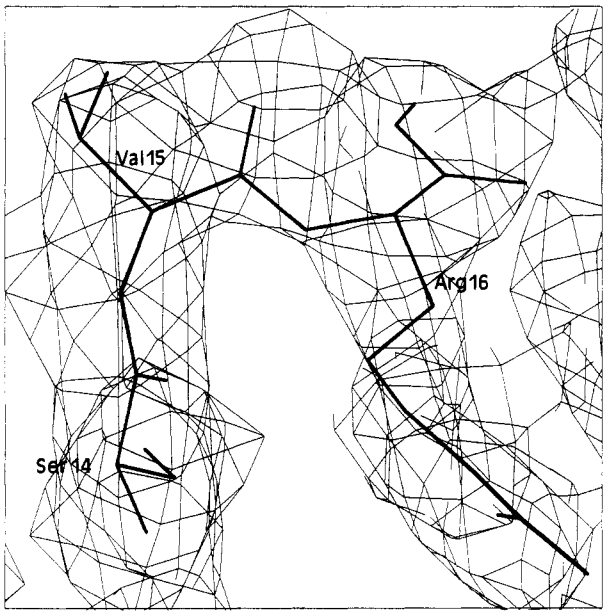

FIGURE 8: Residues Ser14, Val15, and Arg16 from the N-terminal tail of the complex of phosphorylase with glucose, showing the turn centered on Val15. Electron density contours from the $2F_o - F_c$ map are also shown.

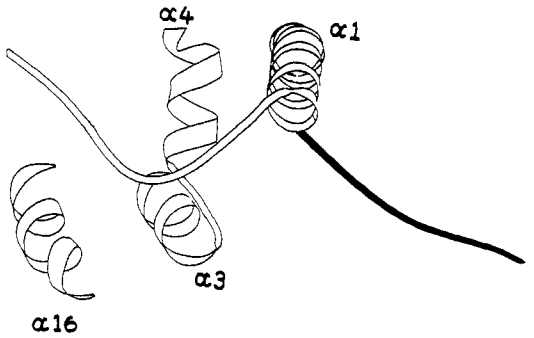

FIGURE 9: N-terminal tail of the T-state enzyme (light ribbon), shown with the helices (α3, α4, and α16) to which it makes hydrogen bonds and van der Waals contacts. The dark ribbon indicates the position of the N-terminal tail observed in phosphorylase *a* (Sprang et al., 1988); it leaves the α1 helix one turn earlier than in T-state phosphorylase *b* [drawn by using RIBBON (Priestle, 1988)].

conformation ends in a turn at Gly20, marking the beginning of the α1 helix. The tail is positioned in a rather broad depression on the surface of the protein, and contacts are formed to residues in the α3, α4, and α16 helices (see Table V) and to a number of water molecules. This stretch of residues is in a completely different location (Figure 9) from that found in both phosphorylase *a* (Sprang et al., 1988) and R-state phosphorylase *b* structures (Barford & Johnson, 1989), where the N-terminal tail interacts with residues from the α2 helix and with residues from the cap region of the other subunit of the enzyme. Interestingly, the α1 helix begins not at Gly20 but at Asn23 in these two structures, and the rest of the tail takes up an extended conformation with some characteristics of a 3_{10} helix. Thus, on going from T-state phosphorylase *b* to phosphorylase *a* (where Ser14 of the N-terminal tail becomes phosphorylated) or R-state phosphorylase *b* (which is crystallized in the presence of sulfate and which mimics the phosphate at Ser14), the changes at the N-terminus are similar; unwinding of the α1 helix by one turn and rotation of the tail by 140°. This movement also requires displacement of part of the C-terminal tail, which in T-state phosphorylase *b* makes contact to the subunit-related cap residues but which is disordered in the phosphorylase *a* and R-state phosphorylase *b* structures. The change in conformation of the N-terminal

Table V: Contacts to N-Terminal Residues for the Four Refined Complexes

(1) Hydrogen Bonds

N-terminal residues	contact residue of phosphorylase	distance (Å)			
		Glc-1-P[a]	glucose	Glc-1-Me-P	2-F-Glc-1-Me-P
Ile13 O	Glu501 OE2		3.0		
Ile13 O	Asn106 ND2			3.3	3.2
Ser14 O	Asn106 ND2	3.0			
Ser14 OG	Glu501 OE2		2.9	3.3	3.2
Arg16 O	Asn106 N	2.9	2.8	3.0	3.2
Arg16 NH1	Asp109 OD2	3.3	3.2	2.8	3.0
Arg16 NH2	Glu501 OE2				3.1
Gly17 O	Asn106 ND2	2.9	2.8	2.8	2.9

(2) van der Waals Contacts

helix	residues
α3	Gln96, Ala103
α4	Glu105, Asn106, Ala107, Asp109
α16	Pro497, Gly498, Glu501, Glu509

[a] For the Glc-1-P complex only, the turn at Val15 is stabilized by a hydrogen bond between the main-chain O of Ser14 and the main-chain N of Arg16 (3.0 Å).

tail may be a response to the increased negative charge on Ser14; in the structures reported here, where Ser14 is unsubstituted, the N-terminal tail is in an anionic environment, but the environment of the N-terminal tail in phosphorylase *a* and R-state phosphorylase *b* is cationic and thus much more favorable for a phosphorylated serine residue (there are 11 acidic residues, and only 7 basic residues, within 15 Å of the Ser14 Cα atom in T-state phosphorylase *b*, while for phosphorylase *a* the ratio is almost reversed, 6 acidic residues and 11 basic residues; note that residues 10–20 were not included in this calculation).

C-Terminus. Pro842, the last residue at the C-terminus, has also been modeled into all four structures. The refined structures indicate that the carboxyl group of Pro842 makes a hydrogen bond to ND2 of the subunit-related cap residue, Asn44. Apart from this last residue, the C-terminus is probably quite flexible, since the conformations of residues 830–841 vary in all of the refined structures, the electron density is sparse, and the *B* factors are very high (100 Å^2).

Discussion

T to R Transition: C-Site Activation. Previous reports on the activation at the C site of glycogen phosphorylase *b* (Barford & Johnson, 1989; Johnson et al., 1990) suggest that the T to R transition is accompanied by two changes: (a) the opening of a channel that allows substrate access to the catalytic site (and concomitantly removes the inhibitor binding site) and (b) the formation of a high-affinity recognition site for phosphate. In particular, the 280s loop, which blocks access to the C site in the native enzyme, becomes disordered and mobile; His571, which makes a hydrogen-bond interaction with Asp283 and also blocks the passage to the C site in the native structure, moves out of the way; and Arg569 swings out from a buried position to one that is much more exposed but is able to interact with phosphate.

The refined structure of the glucose complex shows that binding of glucose at the C site produces none of these changes. Arg569 remains buried, and Asp283 and Asn284 are in the same position where they are found in the native structure and make the same contacts. His571 still blocks access to the C site, and Phe285 continues to form the inhibitor binding site with Tyr613. Indeed, by forming a hydrogen bond to Asn284 of the 280s loop, glucose actively opposes the conformational changes listed above (and thus is described as a T-state-sta-

bilizing inhibitor of the enzyme). This is in agreement with the results obtained for the complex of glucose with glycogen phosphorylase *a* (Sprang et al., 1982).

Most portions of the glucosyl recognition site are retained in the R-state structure (Barford & Johnson, 1989), and the glucosyl portions of the R-state-stabilizing ligands bind to the C site in much the same way as glucose. This is in agreement with the recent (Street et al., 1989) comparisons of kinetic data for the binding of a series of deoxy and deoxyfluoro analogues of glucose and Glc-1-P, which also demonstrated the likelihood of very similar sugar binding sites in both the T- and R-states. In the present work, the phosphorylated ligands induce the C-site alterations described above that lead to opening of the channel to the C site. However, the conformational changes are small and are most likely limited by lattice constraints that restrict the crystalline enzyme from responding fully to the T to R transition. Despite the comparatively small movements and the restraints imposed by the crystal lattice on enzyme conformational changes, the refined structures indicate how R-state-stabilizing ligands induce the displacement of the 280s loop and how I-site ligands that intercalate between Phe285 and Tyr613 prevent such changes from occurring. Thus, with no ligands bound at the I site, the loop is simply pushed downward and out of the C site along the direction of channel 1, formed by the I site. This displacement is different from that observed in the Hept-2-P complex where AMP was also present (Johnson et al., 1990). AMP binds at the I site and thus obstructs movement of the 280s loop along channel 1; instead, it moves to fill the channel vacated by Arg569.

The second change in C-site structure, the formation of a specific binding site for phosphate, is only partially achieved by the binding of these phosphorylated ligands; Asp283, a negatively charged residue, is rotated away from its native position, thus making phosphate binding more favorable. The other change required to complete the creation of the high-affinity phosphate binding site, movement of Arg569 into the C-site cavity, does not occur. However, there are indications that the mobility of Arg569 is increased; the difference Fouriers show quite strong negative density for this residue, and the refined average *B* factors of the side chain are higher than those of the glucose complex. It is possible that Arg569 does visit the C site to interact with the phosphorylated ligands, but the time scale may be too short to be observed by the methods employed here.

Some of the changes observed in the difference Fouriers of the three R-state ligands were not manifested in the final refined structures; thus, the negative density over the 280s loop in the difference Fouriers indicated a large displacement of the loop, but the refined structures only indicate a movement of about 1 Å; similarly, the negative density over Arg569 in the difference Fouriers might suggest that it *has* moved into the phosphate-accessible conformation, but the refined Arg569 conformation is still the buried one. Predictions of protein movement in ligand complexes, made on the basis of difference Fouriers, appear to be overestimated.

Phosphorolytic Catalysis. Enzymes are successful catalysts because they reduce the energy of the transition state of the substrate compared with its ground state. This may occur by stabilization of the transition-state complex or by destabilization of the ground state (or both). Observations emerge from this work which suggest that glycogen phosphorylase employs both mechanisms to catalyze the phosphorolysis of glucosyl phosphates. First, it destabilizes the ground state of the substrate and makes the target bond more susceptible to attack by (a) opening up the angle around C1–O1–P of the ligands to almost 130° and (b) by preventing exo anomeric stabilization of the glucosyl phosphates. Weakening of the exo anomeric effect has been suggested as a mechanism that could be used by enzymes to cleave sugar bonds (Praly & Lemieux, 1987). Second, glycogen phosphorylase stabilizes the transition state. A key feature of the proposed transition state is the close proximity of the PLP cofactor phosphate to the substrate phosphate [see Johnson et al. (1990) for a full discussion of the proposed catalytic mechanism]; this unstable arrangement of negatively charged groups is stabilized in the enzyme by the placement of positively charged groups, such as Lys574 and Arg569, in the vicinity of the phosphate–phosphate bond of the transition-state complex (as observed in the Hept-2-P complex).

The glucosyl portions of the ligands are constrained by intermolecular contacts at the C site to adopt similar binding modes and orientations whether it is glucose or a phosphorylated glucose derivative that binds. As a consequence, formation of the transition state of the substrate Glc-1-P is probably achieved solely by rotation of the phosphate from $\phi = 150°$ (the ground-state binding conformation) to 220°. Conformational calculations (in vacuo) for Glc-1-P at ϕ values of 150° (the bound conformation) and 220° (transition-state conformation) predict hydrogen bonding between the phosphate and the O2 hydroxyl in both cases. However, the transition state is destabilized by over 4 kcal/mol relative to the observed bound conformation, presumably because of the proximity of the phosphate to the O2 hydroxyl in the 220° conformation, which leads to strain in the phosphate bond angle (C1–O1–P). For Hept-2-P, the difference in energy between the two conformations is much less than for Glc-1-P, about 2 kcal/mol. This appears to be a result of destabilization of Hept-2-P conformations close to 120° because of the β-methyl substituent.

For reaction to occur in the enzyme with 2-F-Glc-1-P as substrate, two electrostatically unfavorable interactions must be overcome in the transition-state conformation: the close approach of the substrate phosphate to (1) the cofactor phosphate and (2) to the fluorine at the 2 position. The energy calculations for 2-F-Glc-1-P show a steady increase in energy, to a total of over 5 kcal/mol, as the phosphate moves from the observed bound conformation, $\phi = 110°$, to the transition-state conformation, $\phi = 220°$. This is more than that calculated for Glc-1-P to attain the transition-state conformation and provides a further explanation as to why the reaction rate of 2-F-Glc-1-P is so slow, in addition to the well-established inductive destabilization argument, despite the fact that 2-F-Glc-1-P binds to phosphorylase as tightly as Glc-1-P (Street et al., 1989). The energy calculations cannot explain why Glc-1-Me-P adopts a ϕ value of 180° when bound at the C site, since this conformation is predicted to cost more than 3 kcal/mol.

However, the AM1 results do suggest that Glc-1-P binds to the enzyme in a low-energy conformation (150°) and that energy must be expended to push the phosphate to the transition-state conformation. We believe there are two possible sources of this energy. The first is Arg569, which emerges from a buried position to stabilize the 220° phosphate conformation by ionic and hydrogen-bonding interactions, as observed in the complex with Hept-2-P. But movement of Arg569 into the accessible position does not appear to be the sole stabilizing factor of the transition-state conformation of Glc-1-P. Preliminary results with R-state phosphorylase (where Arg569 is exposed and able to interact with the transition-state phosphate) indicate that Glc-1-P binds in the

ground-state conformation (Barford, Hu, and Johnson, unpublished work). Another factor that might be necessary to push the Glc-1-P phosphate into the correct position for catalysis to occur could be the presence of the other substrate, oligosaccharide, at the C site. This might also explain why the phosphate of Glc-1-Me-P is observed bound at $\phi = 180°$ rather than a more energetically favorable conformation, since maltohexaose was included in the experiment with Glc-1-Me-P but not in the Glc-1-P experiment. Although there is no electron density for oligosaccharide at the C site in the refined Glc-1-Me-P complex, the difference Fourier is noisy and it is possible that the oligosaccharide visits the C site from time to time, thereby exerting an effect that forces the Glc-1-Me-P phosphate into a higher energy conformation.

Protein–Ligand Interactions. Structures of the phosphorylase–ligand complexes show conformational responses by atoms and residues of the macromolecule on binding small molecules. Even in the case of T-state-stabilizing glucose, we observe side-chain movement of one residue (His377) and displacement of a water molecule. But small changes in the ligand structure can produce a completely different response in the protein. Thus, substitution of the α1 hydroxyl of glucose with phosphate to give Glc-1-P produces extensive changes in protein structure when it binds to T-state glycogen phosphorylase *b* (even given the constraints imposed by the crystal lattice). Similarly, small changes in ligand structure can alter the binding mode of the ligand. We have observed this for the binding mode of the phosphate part of phosphorylated glucose derivatives for (1) replacement of a hydroxyl group with a fluoro group (Glc-1-P to 2-F-Glc-1-P), (2) replacement of a hydrogen with a methyl group (Glc-1-P to Hept-2-P), and (3) replacement of a phosphate with a phosphonate (Glc-1-P to Glc-1-Me-P). Conformational energy calculations for the ligand can, to some extent, predict how changes in ligand structure might affect the conformation that binds to the protein. However, without knowledge of the structure of the protein, the task would be made much more difficult. These observations have direct implications for the modeling of ligand–protein interactions, for docking simulations, and for the design of protein inhibitors; not the least of these implications is the necessity in any such study of including information about the structure of the protein and of allowing the structure of the protein to move in response to ligand binding.

ACKNOWLEDGMENTS

We thank R. Acharya, D. Barford, and D. I. Stuart for their contribution to the phosphorylase project, and we thank E. Garman, P. J. Goodford, P. Jeffrey, and E. Y. Jones as well as those mentioned above for their expert advice and helpful discussions; we also thank N. Oikonomakos for supplying glycogen phosphorylase *b* crystals and I. Street for synthesizing and donating two of the phosphorylated compounds (2-F-Glc-1-P and Glc-1-Me-P).

REFERENCES

Barford, D. (1988) D.Phil. Thesis, Oxford University, Oxford, U.K.

Barford, D., & Johnson, L. N. (1989) *Nature 340*, 609–616.

Barford, D., Schwabe, J. W. R., Oikonomakos, N. G., Acharya, K. R., Hajdu, J., Papageorgiou, A. C., Martin, J. L., Knott, J. C. A., Vasella, A., & Johnson, L. N. (1988) *Biochemistry 27*, 6733–6741.

Black, W. J., & Wang, J. H. (1968) *J. Biol. Chem. 243*, 5892–5898.

Boobbyer, D. N. A., Goodford, P. J., McWhinnie, P. M., & Wade, R. C. (1989) *J. Med. Chem. 32*, 1083–1094.

Brown, G. M., & Levy, H. A. (1979) *Acta Crystallogr. B35*, 656–659.

Brunger, A. T. (1988) *J. Mol. Biol. 203*, 803–816.

Brunger, A. T. (1989) *Acta Crystallogr. A45*, 42–50.

Brunger, A. T., Karplus, M., & Petsko, G. A. (1989) *Acta Crystallogr. A45*, 50–61.

Cori, G. T., & Cori, C. F. (1940) *J. Biol. Chem. 135*, 733–756.

Dewar, M. J. S., Zoebisch, E. G., Healy, E. F., & Stewart, J. P. (1985) *J. Am. Chem. Soc. 107*, 3902–3909.

Fersht, A. R., Shi, J.-P., Knill-Jones, J., Lowe, D. M., Wilkinson, A. J., Blow, D. M., Brick, P., Carter, P., Waye, M. M. Y., & Winter, G. (1985) *Nature 314*, 235–238.

Fersht, A. R., Leatherbarrow, R. J., & Wells, T. N. C. (1986) *Trends Biochem. Sci. 11*, 321–325.

Fischer, E. H., & Krebs, E. G. (1962) *Methods Enzymol. 5*, 369–372.

Fischer, E. H., Heilmeyer, L. M. G., Jr., & Haschke, R. H. (1971) *Curr. Top. Cell. Regul. 4*, 211–251.

Fletterick, R. J., & Madsen, N. B. (1980) *Annu. Rev. Biochem. 49*, 31–61.

Fuchs, B., Schleifer, L., & Tartakovsky, E. (1984) *Nouv. J. Chim. 8*, 275–278.

Goodford, P. J. (1985) *J. Med. Chem. 28*, 849–857.

Graves, D. J., & Wang, J. H. (1972) in *The Enzymes* (Boyer, P. D., Ed.) Vol. 7, pp 435–482, Academic Press, New York.

Hajdu, J., Acharya, K. R., Stuart, D. I., McLaughlin, P. J., Barford, D., Oikonomakos, N. G., Klein, H., & Johnson, L. N. (1987) *EMBO J. 6*, 539–546.

Hendrickson, W. A. (1979) *Acta Crystallogr. A35*, 158–163.

Howard, A. J., Gilliland, G. L., Finzel, B. C., Poulos, T. L., Ohlendorf, D. H., & Salemme, F. R. (1987) *J. Appl. Crystallogr. 20*, 383–387.

Johnson, L. N., Jenkins, J. A., Wilson, K. S., Stura, E. A., & Zanotti, G. (1980) *J. Mol. Biol. 140*, 565–580.

Johnson, L. N., Hajdu, J., Acharya, K. R., Stuart, D. I., McLaughlin, P. J., Oikonomakos, N. G., & Barford, D. (1989) in *Allosteric Enzymes* (Herve, G., Ed.) CRC Press, Boca Raton, FL.

Johnson, L. N., Acharya, K. R., Jordan, M. D., & McLaughlin, P. J. (1990) *J. Mol. Biol. 211*, 645–661.

Jones, T. A. (1978) *J. Appl. Crystallogr. 11*, 268–272.

Jones, T. A. (1985) *Methods Enzymol. 115*, 157–171.

Kasvinsky, P. J., Shechosky, S., & Fletterick, R. J. (1978) *J. Biol. Chem. 253*, 9102–9106.

Kasvinsky, P. J., Fletterick, R. J. & Madsen, N. B. (1981) *Can. J. Biochem., 59*, 387–395.

Kirby, A. J. (1983) in *Reactivity and Structure: Concepts in Organic Chemistry*, Springer Verlag, New York.

Klein, H. W., Im, M. J., Palm, D., & Helmreich, E. J. M. (1984) *Biochemistry 23*, 5853–5861.

Lorek, A., Wilson, K. S., Sansom, M. S. P., Stuart, D. I., Stura, E. A., Jenkins, J. A., Zanotti, G., Hajdu, J., & Johnson, L. N. (1984) *Biochem. J. 218*, 45–59.

Madsen, N. B., Avramovic-Zikic, O., Lue, P. F., & Honikel, K. O. (1976) *Mol. Cell. Biochem. 11*, 35–50.

McLaughlin, P. J., Stuart, D. I., Klein, H. W., Oikonomakos, N. G., & Johnson, L. N. (1984) *Biochemistry 23*, 5862–5873.

Monod, J., Wyman, J., & Changeux, J.-P. (1965) *J. Mol. Biol. 12*, 88–118.

Narendra, N., & Viswamitra, M. A. (1984) *Curr. Sci. 53*, 1018–1020.

Narendra, N., Seshadri, P., & Viswamitra, M. A. (1984) *Acta Crystallogr. C40*, 1338–1340.

Newgard, C. B., Hwang, P. K., & Fletterick, R. J. (1989) *Crit. Rev. Biochem. Mol. Biol. 24*, 69–99.
Oikonomakos, N. G., Melpidou, A. E. & Johnson, L. N. (1985) *Biochim. Biophys. Acta 832*, 248–256.
Oikonomakos, N. G., Johnson, L. N., Acharya, K. R., Stuart, D. I., Barford, D., Hajdu, J., Varvill, K. M., Melpidou, A. E., Papageorgiou, T., Graves, D. J., & Palm, D. (1987) *Biochemistry 26*, 8381–8389.
Oikonomakos, N. G., Acharya, K. R., Stuart, D. I., Melpidou, A. E., McLaughlin, P. J., & Johnson, L. N. (1988) *Eur. J. Biochem. 173*, 569–578.
Praly, J. P., & Lemieux, R. U. (1987) *Can. J. Chem. 65*, 213–223.
Priestle, J. P. (1988) *J. Appl. Crystallogr. 21*, 572–576.
Sansom, M. S. P. (1983) D.Phil. Thesis, Oxford University, Oxford, U.K.
Sansom, M. S. P., Stuart, D. I., Acharya, K. R., Hajdu, J., McLaughlin, P. J., & Johnson, L. N. (1985) *J. Mol. Struct.: THEOCHEM 123*, 3–25.
Sprang, S. R., & Fletterick, R. J. (1979) *J. Mol. Biol. 131*, 523–551.
Sprang, S. R., Goldsmith, E. J., Fletterick, R. J., Withers, S. G., & Madsen, N. B. (1982) *Biochemistry 21*, 5364–5371.
Sprang, S. R., Acharya, K. R., Goldsmith, E. J., Stuart, D. I., Varvill, K., Fletterick, R. J., Madsen, N. B., & Johnson, L. N. (1988) *Nature 336*, 215–221.
Street, I. P., Armstrong, C. R., & Withers, S. G. (1986) *Biochemistry 25*, 6021–6027.
Street, I. P., Rupitz, K., & Withers, S. G. (1989) *Biochemistry 28*, 1581–1587.
Suguwara, Y., & Iwasaki, H. (1984) *Acta Crystallogr. C40*, 389–393.

Analysis of Sequence Homologies in Plant and Bacterial Pyruvate Phosphate Dikinase, Enzyme I of the Bacterial Phosphoenolpyruvate: Sugar Phosphotransferase System and Other PEP-Utilizing Enzymes. Identification of Potential Catalytic and Regulatory Motifs[†,‡]

David J. Pocalyko,[§] Lawrence J. Carroll,[§] Brian M. Martin,[⊥] Patricia C. Babbitt,[∥] and Debra Dunaway-Mariano*[,§]

Department of Chemistry and Biochemistry, University of Maryland, College Park, Maryland 20742, Molecular Neurogenetics Unit, Clinical Neuroscience Branch, National Institute of Mental Health, Bethesda, Maryland 20892, and Department of Pharmaceutical Chemistry, University of California, San Francisco, California 94143

Received April 10, 1990; Revised Manuscript Received July 30, 1990

ABSTRACT: In this paper we report the amino acid sequence of pyruvate phosphate dikinase (PPDK) from *Bacteroides symbiosus* as determined from the nucleotide sequence of the PPDK gene. Comparison of the *B. symbiosus* PPDK amino acid sequence with that of the maize PPDK [Matsuoka, M., Ozeki, Y., Yamamoto, N., Hirano, H., Kamo-Murakami, Y., & Tanaka, Y. (1988) *J. Biol. Chem. 263*, 11080] revealed long stretches of homologous sequence (>70% identity), which contributed to an overall sequence identity of 53%. The circular dichrosim spectra, hydropathy profiles, and calculated secondary structural elements of the two dikinases suggest that they may have very similar tertiary structures as well. A comparison made between the amino acid sequence of the maize and *B. symbiosus* dikinase with other known protein sequences revealed homology, concentrated in three stretches of sequences, to a mechanistically related enzyme, enzyme I of the *Escherichia coli* PEP:sugar phosphotransferase system [Saffen, D. W., Presper, K. A., Doering, T. L., Roseman, S. (1987) *J. Biol. Chem. 262*, 16241]. It is proposed that (i) these three stretches of sequence constitute the site for PEP binding and catalysis and a possible site for the regulation of enzymatic activity and (ii) the conserved sequences exist in a third mechanistically related enzyme, PEP synthase.

Pyruvate phosphate dikinase (PPDK)[1] catalyzes the reversible phosphorylation of pyruvate and orthophosphate with the β- and γ-phosphoryl groups of a single molecule of ATP (Reeves et al., 1968; Evans & Wood, 1968):

$$\text{Ade } \overset{\beta\gamma}{\text{PPP}} + \text{P}_\text{i} + \text{pyruvate} \rightleftharpoons \text{Ade P} + \overset{\gamma}{\text{PP}_\text{i}} + \overset{\beta}{\text{PEP}}$$

The enzyme has been found in a variety of unicellular organisms and in C_4 and some Crassulacean acid metabolism plants (Reeves, 1968; Reeves et al., 1968; Evans & Woods, 1968; Benzimam & Palgi, 1970; Hatch & Slack, 1968; Kluge & Osmond, 1971). In *Entamoeba histolytica* and *Bacteroides symbiosus* where pyruvate kinase is absent, PPDK functions in the direction of ATP synthesis. In *Propionibacterium shermanii*, *Acetobacter xylinum*, the photosynthetic bacterium, *Rhodospirillum rubrum*, and the C_4 and Crassulacean acid

[†] This work was supported by NIH Grants GM-36260 and GM-28688.
[‡] The nucleic acid sequence in this paper has been submitted to GenBank under Accession Number J05295.
* To whom correspondence should be addressed.
[§] University of Maryland.
[⊥] National Institute of Mental Health.
[∥] University of California.

[1] Abbreviation ATP, adenosine 5′-triphosphate; PEP, phosphoenolpyruvate; PP_i, inorganic pyrophosphate; P_i, orthophosphate; EP, phosphoenzyme; EPP, pyrophosphoenzyme; ADP, adenosine 5′-diphosphate; AMP, adenosine 5′-monophosphate; PPDK, pyruvate phosphate dikinase; PTS, PEP:sugar phosphotransferase system; BRFP, bifunctional regulatory protein; HPLC, high-pressure liquid chromatography; CD, circular dichroism.

0006-2960/90/0429-10757$02.50/0